

**Reuse potential of architectural glass
experimental study on the strength of used window glazing**

Cupac, Jagoda; Datsiou, Kyriaki Corinna; Louter, Christian

DOI

[10.1007/s40940-024-00267-y](https://doi.org/10.1007/s40940-024-00267-y)

Publication date

2024

Document Version

Final published version

Published in

Glass Structures and Engineering

Citation (APA)

Cupac, J., Datsiou, K. C., & Louter, C. (2024). Reuse potential of architectural glass: experimental study on the strength of used window glazing. *Glass Structures and Engineering*. <https://doi.org/10.1007/s40940-024-00267-y>

Important note

To cite this publication, please use the final published version (if applicable).
Please check the document version above.

Copyright

Other than for strictly personal use, it is not permitted to download, forward or distribute the text or part of it, without the consent of the author(s) and/or copyright holder(s), unless the work is under an open content license such as Creative Commons.

Takedown policy

Please contact us and provide details if you believe this document breaches copyrights.
We will remove access to the work immediately and investigate your claim.



Reuse potential of architectural glass: experimental study on the strength of used window glazing

Jagoda Cupac¹ · Kyriaki Corinna Datsiou² · Christian Louter³

Received: 19 March 2024 / Accepted: 25 June 2024
© The Author(s) 2024

Abstract Glass is a highly durable and infinitely recyclable material, yet in practice only a small portion of architectural glass products re-enters the value chain after its first use. An increasing rate of energy retrofits of the EU building stock will result in replacement of 85% of existing windows in near future; in the current linear glass supply chain, this will generate large amounts of glass waste. Despite high recycling rates of container glass in Europe, window glazing is very rarely recycled into new glazing, and reuse is almost entirely unexplored. For aged glazing to be reused in construction, better knowledge of its surface quality and structural performance is needed. The main objective of this paper is to explore the effects of ageing and exposure to indoor and outdoor environment on the strength of glass. A comparative investigation is undertaken to evaluate the strength and surface quality of the internally, externally and cavity-facing glass surfaces of insulating glass units (IGUs) after 30 years of use in a building envelope in the Netherlands. The glass panes are separated from the IGU assembly and cut into specimens for microscopy and coaxial double ring tests. The study shows that the visual quality is best preserved on

the cavity-facing surface, consequently exhibiting the highest bending strength. The internally and externally facing surfaces, with visibly more extensive damage, exhibited similarly lower strengths at low probabilities of failure. When compared to the design strength of new annealed glass acc. to EN 16612, all the surfaces showed a reuse potential, with considerable bending strength.

Keywords Glass strength · IGU · Aged glass · Reuse

1 Introduction

Glass is a highly durable and infinitely recyclable material, yet in practice only a small portion of architectural glass products re-enters the value chain after its first use. In view of the European Green Deal and the 2050 decarbonisation objectives (European Commission 2020), 85% of the existing window stock, with the average insulation performance of only $U_w = 3.4 \text{ W}/(\text{m}^2\text{K})$, will require refurbishment or replacement (European Commission 2018). In the current linear glass supply chain, this will generate large amounts of glass waste. Despite high recycling rates of container glass in Europe, flat glass used for window glazing is very rarely recycled into new glazing, and reuse is almost entirely unexplored.

For instance, a study on recycling of flat glass in Germany showed that almost 90% of flat glass waste generated in the building sector is recycled (Rose et al.

J. Cupac (✉)
Technische Universität Dresden, Dresden, Germany
e-mail: jagoda.cupac@tu-dresden.de

K. C. Datsiou
University of Hertfordshire, Hatfield, UK

C. Louter
Delft University of Technology, Delft, The Netherlands

2019). However, only 11% is returned to the flat glass production, while the remaining glass recycle (cullet) is downcycled into container glass, mineral wool, glass beads and glass flour. Hartwell et al. (2023) identified similar trends mapping the UK flat glass value chain, where end-of-life building glass returns to the container glass market, or, in case of lower quality cullet, to the aggregates market or glass beads. In Sweden, which has well-developed closed-loop supply chains for many materials, only 1% of flat glass is processed in a closed loop (Forslund and Björklund 2022), while in the Netherlands a higher percentage of 7.5% is achieved, resulting from the establishment of the nationwide glass collection initiative “Vlakglas Recycling Nederland” (Bristogianni and Oikonomopoulou 2023). Focusing more specifically on insulating glass units (IGUs), Geboes et al. (2023) analysed the level of application of circular practices in the Belgian regions of Flanders and Brussels, including recycling, reuse, repair and repurpose. Even the pre-consumer IGUs, originating from order surpluses or damage during installation or transport, are typically downcycled to container glass, glass wool insulation or foam glass, due to possible contamination of the glass with nickel sulphide from the metal spacer bars. Such contamination, once introduced into the float line furnace, can take several days of lost production before passing through the system. When left undetected, it can cause spontaneous glass breakage after manufacturing and thermal tempering. Most of the post-consumer flat glass waste from IGUs is used in low value applications, i.e. as filler in recycled aggregates for concrete production. The study mentions an instance of IGU glazing repurposed as indoor partitioning wall, but states that repair and reuse, and even closed loop recycling, are still absent in the Flemish and Brussels construction practices. IGU repair remains a niche market, demonstrated only through a couple of projects, such as Empire State Building in New York and One Triton Square in London (ibid.). In 2021, Dutch company GSF Glasgroep launched a circular IGU made of one uncoated glass pane obtained from disassembly of end-of-life IGUs, and one virgin coated glass (van Nieuwenhuijzen et al. 2023). Today, the company also offers a fully circular IGU made from two reused and uncoated glass panes, with a maximum U value of $2.7 \text{ W}/(\text{m}^2\text{K})$. The maximum U value of the former, 50% circular IGU, is $1.1 \text{ W}/(\text{m}^2\text{K})$ (GSF Glasgroep 2024). A recent built example of glass reuse is the Natural Pavilion designed

by the architectural firm DP6 architectuurstudio for the Floriade Expo 2022 in Almere, the Netherlands. The project reused single glazing from a government building in the Hague, adapting the design of the building to the size of the reclaimed glass panels (DP6 architectuurstudio 2022; Veer et al. 2023).

IGUs are mainly being replaced due to degradation of the primary seal which results in significant reduction of thermal performance and may lead to condensation in the air cavity, with a negative impact on the transparency of the glazing (Fig. 1). The expected service life of an IGU assembly is only 25 years, due to the limited durability of the seal, while the expected service life of a single glass pane is 60 + years (CWCT 2021).

For aged glazing to be reused in construction, better knowledge of its surface quality and structural performance is needed. The strength of (new) glass is governed by the condition of its surface, i.e. the density and depth of flaws which arise during the manufacturing process, and subsequent processing, handling and installation. Additional damage accumulates from exposure to wind-borne debris, human impact or cleaning during the service life, resulting in reduced strength of aged glass. The reduction of glass strength due to ageing has been investigated in a limited number of studies. Overend and Louter (2015) analysed naturally weathered annealed glass after 20 years of service life as single glazed windows in a low rise building in Norfolk, UK. The glass was tested in a coaxial double ring (CDR) setup, with the loading ring diameter $D_L = 15 \text{ mm}$, and the supporting ring diameter $D_S = 48 \text{ mm}$, following the ASTM recommendations (ASTM C1499-09 2013). The tests were performed under inert conditions, at a stress rate of approximately 2.3 MPa/s . The mean strength of the aged glass amounted to $\sigma_{f,0.5} = 101.2 \text{ MPa}$ or 70% of the strength of new glass, tested in the same study. However, at lower probabilities of failure, which correspond with the design value commonly used in engineering applications, the strength level of aged glass reached only 24% of the strength of new glass ($\sigma_{f,0.008} = 18.7 \text{ MPa}$). In a subsequent study of artificial ageing methods for glass, Datsiou and Overend (2017a) performed additional destructive tests on the aged glass sourced from the same building. The CDR tests were performed on larger specimens ($D_L = 51 \text{ mm}$; $D_S = 127 \text{ mm}$) under ambient conditions, with increased stress rate of 20 MPa/s to minimise the influence of sub-critical crack growth. The



Fig. 1 Effect of condensation in the IGU cavity on the transparency of the glazing; Centre Pompidou, Paris

study showed that the glass suffered 73–85% strength reduction at lower probabilities of failure ($\sigma_{f,0.008} = 10.0\text{--}18.4$ MPa), with respect to new glass tested under the same conditions. In 2023, 50⁺-year-old monolithic annealed glass, originating from the renovation of a high-rise office building in the Hague, was tested by Veer et al. (2023). The glass was installed in the outer skin of a double skin façade, exposed to relatively high wind loads and abrasion due to the proximity to the sea and major roads and the height of the building. Two sample sizes were tested in CDR setup to examine the size effect, with (i) $D_L = 72$ mm; $D_S = 150$ mm, and (ii) $D_L = 180$ mm; $D_S = 250$ mm, selected in accordance with the ASTM C1499-09 (2013). The specimens were covered with a self-adhesive plastic foil on both sides, to contain the fragments after fracture and limit the effects of stress corrosion. The tests were conducted at a nominal stress rate of 7.6 MPa/s and 4.2 MPa/s, for the small and large specimens, respectively. Both exterior and interior surfaces of the aged specimens were tested, as well as new glass, on both air and tin side. The study found an approximately 50% reduction in the mean strength of the weathered glass, compared to

new glass, and a minimum strength of about 30 MPa at a probability of failure of 2–5%. No significant size effect was observed for the exterior surface strength, suggesting that the density of the surface damage is so high and uniformly distributed that the probability of detecting a critical defect does not significantly depend on the size of the tested surface. However, for the interior surface, the tests on larger specimens resulted in significantly lower strength, relative to the smaller specimens, indicating a lower density of more singular defects.

In 2023, Rota et al. (2023) published a study proposing a quality protocol for the reuse of end-of-life window glazing, including the assessment of the surface quality of 43 IGUs collected in residential buildings in Belgium after 28–41 years of service life. The IGUs were disassembled, and the glass tested in a CDR setup according to the ASTM C1499-09 (2013). Several specimen sizes were investigated, including different D_L/D_S combinations (20 mm/80 mm, 40 mm/80 mm and 80 mm/150 mm), with a constant nominal stress rate of 2 MPa/s. The study focused on the strength on annealed uncoated glass, with an additional series of thermally tempered glass (tempered after ageing).

The surface quality was pre-assessed with a commercially available optical scanner, fitted on a manufacturing IGU line, and sorted into quality levels—QL1, QL2, QL3—according to the number of detected spot and linear defects. The strength data was analysed with respect to the predetermined quality level and the tested IGU surface (Fig. 2, surfaces S1–S4). The glass classified as Q1 exhibited a strength value comparable to new glass, with the expected decrease in strength observed for the lower quality glass. The comparison of the characteristic bending strength (at a 5% probability of failure) of different IGU surfaces led to a surprising outcome—the cavity facing surfaces S2 and S3 resulted in the lowest strength ($\sigma_{f,0.05,S2} = 45$ MPa; $\sigma_{f,0.05,S3} = 44$ MPa), followed by the externally and internally facing surfaces S1 and S4 ($\sigma_{f,0.05,S1} = 48$ MPa; $\sigma_{f,0.05,S4} = 54$ MPa). No correlation was found between the lifespan of the IGUs and its mechanical performance. With respect to the specimen size and the loading ring/supporting ring combinations, the 80 mm/150 mm combination yielded the highest number of valid tests (fracture origin located within or directly under the loading ring). The results obtained for the tempered *aged* glass, compared to the tempered *new* glass, suggest that thermal tempering could be used to improve the strength of aged post-consumer glass.

In the most recent study by Stuurstraat (2023), 36-year-old IGUs from an apartment building in Amstelveen, the Netherlands, were destructively tested in a CDR setup ($D_L = 60$ mm; $D_S = 120$ mm). A total of 406 specimens of uncoated annealed glass were tested under ambient conditions at a stress rate of 20 MPa/s.

Analysis of the strength data at low probabilities of failure of 0.8% resulted in the highest strength for the externally facing surface ($\sigma_{f,0.008,S1} = 24.1$ MPa), followed by the internally facing surface ($\sigma_{f,0.008,S4} = 16.8$ MPa), and the lowest strength for the cavity facing surfaces ($\sigma_{f,0.008,S2} = 11.4$ MPa; $\sigma_{f,0.008,S3} = 14.9$ MPa).

Existing studies demonstrate that aged glass exhibits reduced bending strength when compared to new glass, however, depending on the application, it still presents a significant potential for reuse. The observed strengths vary greatly, as well as the testing methodologies, making direct comparison and derivation of design strengths difficult. A larger database of strength test results, examining a wider variety of samples, with different origin and level of exposure, is necessary to eventually arrive at a uniform approach to testing and data processing for aged glass, and finally obtain design values which would facilitate its reuse.

The main objective of this paper is to further explore the effects of ageing and exposure to indoor and outdoor environment on the strength of glass. A comparative investigation is undertaken to evaluate the strength and surface quality of the internally, externally, and cavity-facing glass surfaces of insulating glass units after 30 years of use in a building envelope in the Netherlands. The following section describes the evaluation methodology, including the IGU disassembly and cutting, microscopy, strength characterisation and statistical analysis of strength data. The results are discussed in Sect. 3, with the conclusions of the study outlined in Sect. 4.

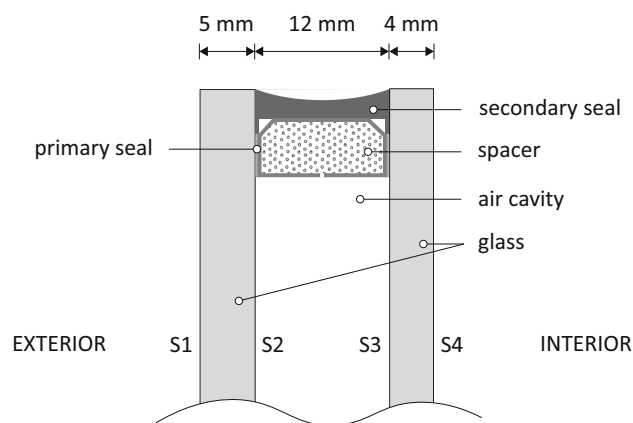


Fig. 2 IGU composition

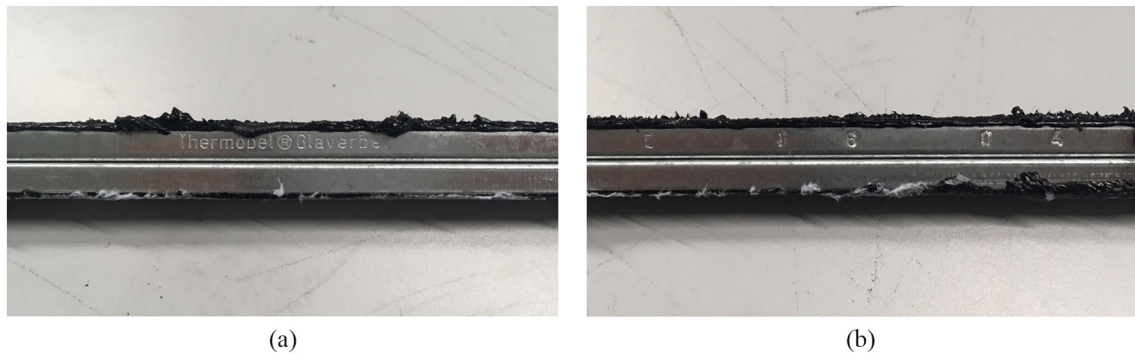


Fig. 3 IGU spacer indicating: **a** the product name (Thermobel®Glaverbel); **b** the production code (5 86 04)

2 Evaluation of used glazing unit

The IGUs investigated in this study were retrieved from a refurbishment project in Vleuten, a neighbourhood in the city of Utrecht, the Netherlands, in 2016. They had been installed in one-storey high single dwellings. The IGUs have a relatively small dimension of 252 mm × 725 mm. They had been used in transom windows (fanlight), typically installed above openable windows or doors to provide additional light.

Seven IGUs were initially analysed with Bohle GlassBuddy®, to determine the glass thickness, configuration of panes, any coatings, interlayers (i.e. laminated glass), and their exact position in the IGU. The configuration of the IGUs, schematically shown in Fig. 2, includes two annealed float glass panes, with a nominal thickness of 4 mm and 5 mm. According to the refurbishment contractor, the IGUs were installed with the thicker 5 mm pane facing the exterior. No coatings were detected on any of the glass surfaces. The two panes were separated with a spacer and bonded with a sealant, enclosing a 12 mm wide air cavity. Furthermore, the measuring device Bohle TinCheck® was used to identify the tin bath side of the glass. No consistency was found in the placement of the tin/air side relative to the position of the glass surface within the IGU. Glass surfaces are numbered from the exterior to the interior, as shown in Fig. 2 (surfaces S1–S4).

According to the product name, Thermobel®Glaverbel, and the five-digit code imprinted on the spacer (Fig. 3), the IGUs had been produced by AGC Kempenglas in Belgium between January and May 1986. The IGUs had, therefore, been in use for about 30 years. An example of the spacer code is shown in Fig. 3b. The first digit (5) indicates the

factory, the second and third (86)—the year, and the fourth and fifth digits (04)—the month of production. The interpretation of the code was obtained through personal communication with the manufacturer.

2.1 IGU disassembly and cutting

To perform the experimental investigation on different surfaces of the IGUs, the units were disassembled, and the glass panes cut into test specimens for subsequent microscopy evaluation and coaxial double ring tests. The units were disassembled by, firstly, removing the secondary seal with a joint knife to provide access to the primary seal (Fig. 4a). With a box cutter, the glass panes and the spacer were then separated by cutting through the primary seal (Fig. 4b). The glass panes were cleaned with a cleaning agent (REINEX GLAS Reiniger) and a dry cloth and handled carefully to prevent additional damage.

After the disassembly, the glass panes were cut into specimens of 100 mm × 100 mm, according to the EN 1288-5 standard for coaxial double ring tests on flat specimens with small test surface areas (CEN 2000). The standard specifies a method for determining the comparative bending strength of glass, as intended in this study, using relatively small specimens, which maximises the number of specimens obtained from a single pane and results in a larger data set for the statistical analysis. The surface of the glass pane was marked for cutting, discarding the edges of the pane, which were likely damaged while cutting through the primary seal (Fig. 5). The glass was manually scored along the cutting lines with a diamond cutter and cut by applying tensile stress along the scored lines. Series



Fig. 4 IGU disassembly: **a** removal of the secondary seal; **b** cutting through primary seal

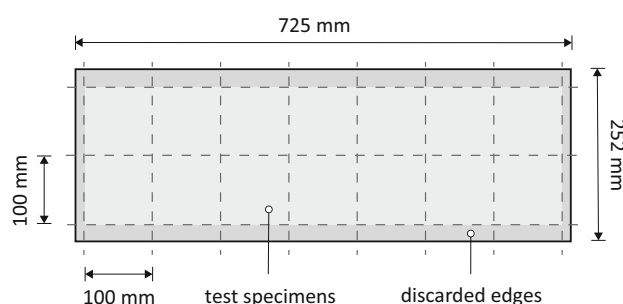


Fig. 5 Cutting scheme for obtaining the test specimens from the disassembled glass pane

of maximum 14 specimens were obtained from each glass pane, reduced in some cases to 12–13, due to the damage which occurred in the disassembly and/or cutting process. The thickness of each specimen was measured at 4 points on the edges, and the average thickness was determined per specimen. The number of obtained specimens tested in each series, and their average thickness, is listed in Table 2.

2.2 Microscopy

Micrographs of each glass surface were recorded for all the specimens to obtain qualitative images of the surface, determine the comparative level of surface damage and detect potential critical flaws (Fig. 6a). Only the central area of 20 mm × 20 mm (enclosing the test area under the loading ring) was examined (Fig. 6c) with an automated digital microscope Zeiss Smart Zoom 5 at a magnification level of 100x. It should be noted that the micrographs provide only a two-dimensional image of

the glass surface, without the information on the depth of the detected flaws.

2.3 Strength characterisation

The specimens were subjected to coaxial double ring tests (Fig. 6b), following the procedure set in EN 1288-5 (CEN 2000). The tested IGU surface (Fig. 2) for each series/glass pane (S1/S2 for the external pane, S3/S4 for the internal pane) varied according to the test matrix shown in Table 1. The test series are detailed in Table 2, listing the tested surface, detected tin or air side, average thickness, number of tested specimens and valid tests, and applied nominal stress rate.

For the specimen size of 100 mm × 100 mm, a corresponding loading device R45 was applied, with the radius of the loading ring $r_1 = 9$ mm, and the radius of the supporting ring $r_2 = 45$ mm (Fig. 6c). The tests were performed under ambient conditions (22 ± 2 °C, 36–58% RH), and were force controlled, loading the

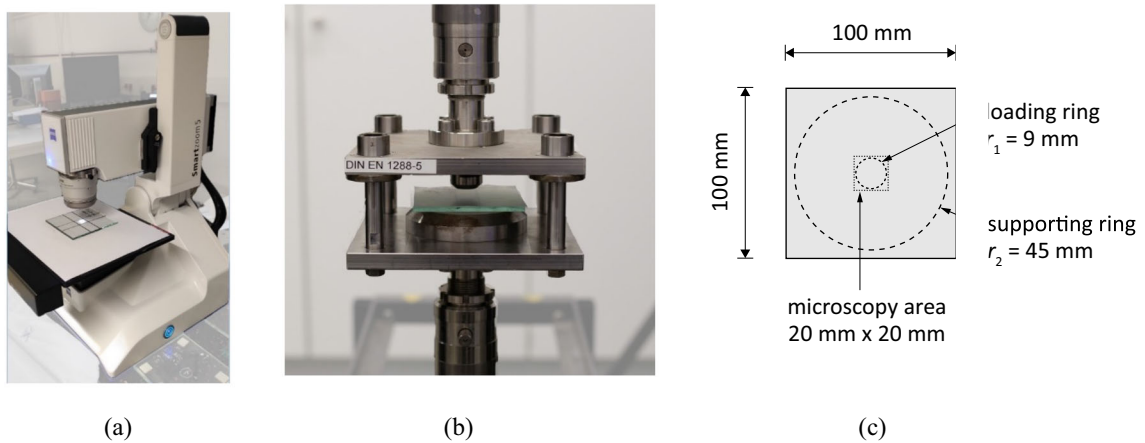


Fig. 6 Test specimen in **a** the microscopy and **b** the coaxial double ring test setup; **c** loading and supporting ring and microscopy area marked on the test specimen

Table 1 Test matrix

IGU	Tested IGU surface			
	S1	S2	S3	S4
IGU1	✓	–	✓	–
IGU2	✓	–	–	✓
IGU3	–	✓	–	✓
IGU4	✓	–	✓	–
IGU5	–	✓	–	✓
IGU6	✓	–	–	✓
IGU7	✓	–	–	✓

specimens to failure at a nominal stress rate of 2 MPa/s (except for one series, where a higher stress rate of 20 MPa/s was applied). The corresponding load rate was adjusted for each series, according to the average thickness of the specimens.

An adhesive film was applied on the upper surface of the specimen, facing the loading ring, to retain the fragments after fracture and facilitate identification of the fracture origin. Only strength data from specimens with fracture origins located within or directly under the loading ring were considered valid and were subsequently statistically analysed. Among these, approximately 25% of the valid tests failed directly under the loading ring. Although deviations from the expected equi-biaxial stress state are known to occur at the interface with the loading ring due to contact effects, these become significant as non-linear effects (deflection / thickness ratio) increase, making them more relevant

for thin toughened glass (Datsiou and Overend 2017b). Consequently, contact effects were not considered in this study.

2.4 Statistical analysis of strength data

Initially, the fracture strength data, σ_f , were converted to a time-equivalent strength, $\sigma_{f,eq}$, to address the varying occurrence of sub-critical crack growth as specimens failed at different times to failure, t_f . Specifically, the ramp stress history during the coaxial double ring tests was converted to a constant stress for an equivalent time period of $t_{eq} = 60s$, following Brown’s integral as follows (Brown 1969):

$$\int_0^{t_f} \sigma_f^n(t) dt = \int_0^{t_{eq}} \sigma_{f,eq}^n dt \tag{1}$$

Table 2 Test series

Series	IGU surface	Tin or air side	Average thickness [mm]	Number of tested specimens	Number of valid tests	Nominal stress rate [MPa/s]
IGU1-S1T	S1	Tin	4.82	13	6	2
IGU1-S3T	S3	Tin	3.91	14	12	2
IGU2-S1A	S1	Air	4.81	13	8	2
IGU2-S4A	S4	Tin	3.81	14	9	2
IGU3-S2A	S2	Air	4.80	14	5	2
IGU3-S4A	S4	Air	3.79	13	6	20
IGU4-S1T	S1	Tin	4.84	14	8	2
IGU4-S3A	S3	Air	3.81	14	5	2
IGU5-S2T	S2	Tin	4.80	14	6	2
IGU5-S4T	S4	Tin	3.84	12	5	2
IGU6-S1A	S1	Air	4.87	14	8	2
IGU6-S4A	S4	Air	3.79	14	8	2
IGU7-S1A	S1	Air	4.90	13	5	2
IGU7-S4T	S4	Tin	3.84	14	8	2
Total number of tested specimens/valid tests:				190	99	

where $n = 16$ is the static fatigue constant for normal environmental conditions, that is commonly used in glass strength analysis (Haldimann 2006).

The time-equivalent fracture strength data were subsequently statistically analysed and fitted to a 2-parameter Weibull distribution Eq. (2). For this, a weighted least squares regression method was employed in conjunction with Faucher and Tyson's weight function and Hazen's probability estimator, following the procedure outlined in Datsiou and Overend (2018). This method was preferred for its effectiveness for small sized glass strength data, as it produces a better goodness-of-fit and was found to provide more conservative estimates at lower probabilities of failure compared to other manual calculation and computational methods.

$$P_f = 1 - \exp\left(-\left(\frac{\sigma_{f,eq}}{\theta}\right)^\beta\right) \quad (2)$$

where P_f is the probability of failure, β is the shape factor and θ is the scale factor of the Weibull distribution.

The Anderson Darling (AD) goodness of fit p_{AD} (Eq. 3) is commonly used in glass statistics to assess whether the Weibull distribution provides a good fit to the fracture data under consideration (Datsiou and

Overend 2018). This method employs a weight function giving greater emphasis to the upper and lower tail of the cumulative distribution function which is essential in glass statistics as low probabilities of failure are typically considered for design purposes. The AD goodness of fit was therefore selected in this study for a chosen significance level of $\lambda = 0.05$.

$$p_{AD} = \frac{1}{1 + \exp(-0.1 + 1.24 \cdot \ln(AD^*) + 4.48 \cdot AD^*)} \quad (3)$$

where

$$AD^* = \left(1 + \frac{0.2}{\sqrt{n}}\right) \cdot AD^2 \text{ and } AD^2 = -n \sum_{i=1}^n \frac{(2i-1)}{n} [\ln(P_f(\sigma_i)) + \ln(1 - P_f(\sigma_{n+1-i}))]$$

where i is the index of ascending order and n is the sample size.

Strength data were subsequently derived for the design and mean probabilities of failure to compare results across different series. A design probability of failure of $P_f = 0.008$ was selected in this study following the recommendations of ASTM E1300-16 (2016)

but any other appropriately low probability of failure could be used.

3 Results and discussion

3.1 Externally facing glass surface

Microscopy of the externally facing glass surface (S1 in Fig. 2) revealed extensive damage, predominantly pits and some scratches (Fig. 7). The damage can be attributed to the long-term exposure of the surface to the external environment. Pits were likely caused by the impact of airborne projectiles, as well as transport, installation and cleaning processes that were likely also responsible for the observed scratches. This is consistent with previous observations in Datsiou and Overend (2017a), and more recently in Stuurstraat (2023).

Five series of test data were analysed for externally facing glazing derived from five distinct IGUs (Table 1). Fracture data were acquired from the tin side of glass for series IGU1-S1T and IGU4-S1T while the remaining series (IGU2-S1A, IGU6-S1A and IGU7-S1A) featured data from the air side of the glass. All series showed acceptable goodness of fit to the Weibull distribution (Table 3), exceeding the 5% significance level selected for this study. The sole exception was IGU4-S1T which exhibited poor goodness of fit. The fracture data for this series are arranged in two distinct groups (Fig. 8), suggesting that the data from each group arose from different flaw typologies. Consequently, it is expected that this series would be better described by a bi-modal Weibull distribution.

The cumulative distribution functions (CDFs) for all series exhibited a consistent trend, with each curve being nearly parallel to one another (Fig. 8). Indeed, it was found that the shape factor, β , which governs the gradient of the CDF of the Weibull distribution, was low and very similar across all series, within the range of $3.51 \leq \beta \leq 4.1$. This indicates the wide spectrum of the obtained fracture strength data and closely matches previous findings on the shape factor of naturally aged glass in Datsiou and Overend (2017a). Low shape factors are expected for naturally aged glazing as it is subject to uncontrolled and random flaw inducing mechanisms during its service life.

Close agreement was observed in CDFs for series IGU1-S1T and IGU4-S1T, both of which featured fracture strength data on the tin side of glass. Similarly for

the air side data, series IGU2-S1A and IGU6-S1A were closely aligned. A small deviation was observed for series IGU7-S1A which, however, converged with the other two for strengths at low probabilities of failure. It is evident that the tin side series consistently resulted in lower strength compared to the air side. Overall, the strength of glass varied between $19.9 \leq \sigma_{f,0.008} \leq 27.4$ MPa at low probabilities of failure ($P_f = 0.008$) with a coefficient of variation of 13.8% while the mean fracture strength ranged between $60 \leq \sigma_{f,0.5} \leq 76.1$ MPa with a coefficient of variation of 19%.

3.2 Cavity facing glass surfaces

Micrographs recorded on the cavity facing glass surfaces (S2 and S3 in Fig. 2), exhibited nearly defect free conditions. Figure 9 shows two micrographs of the cavity facing surface, where a rare instance of damage was detected: a widely spread scratch on surface S2 (Fig. 9a, specimen IGU5-S2T-4) and pits on surface S3 (Fig. 9b, specimen IGU4-S3A-13). Given that the cavity facing surfaces were protected during the lifetime of the IGU, the damage might have been caused during assembly or disassembly of the units. In subsequent destructive tests, the observed flaws did not initiate the fracture of the specimens, indicating that a more severe flaw was present on the surface, but was not detected through surface microscopy.

The fracture strength of a total of four series of cavity facing glazing were investigated for four distinct IGUs (Table 1). For each cavity facing surface, namely S2 and S3 of the external and internal glass panel (Fig. 2), two series were tested (IGU3-S2A & IGU5-S2T for S2 and IGU1-S3T & IGU4-S3A for S3). Among those, one series pertained to the air side of glass while the other to the tin side of glass.

All series successfully met the goodness of fit criteria for the Weibull distribution (Table 4). However, significant variation was observed in the CDFs among the tin and air side series for both S2 and S3 surfaces (Fig. 10). Specifically, series IGU3-S2A and IGU1-S3T demonstrated an increased shape factor of 6.4 and 7.8 respectively. This aligns with findings for as-received / non-aged glass (Overend and Louter 2015) and is a reflection of the narrow spread of the fracture strength data.

However, low shape factors of 2.1 and 3.3 were found for series IGU4-S3A and IGU5-S2T which were

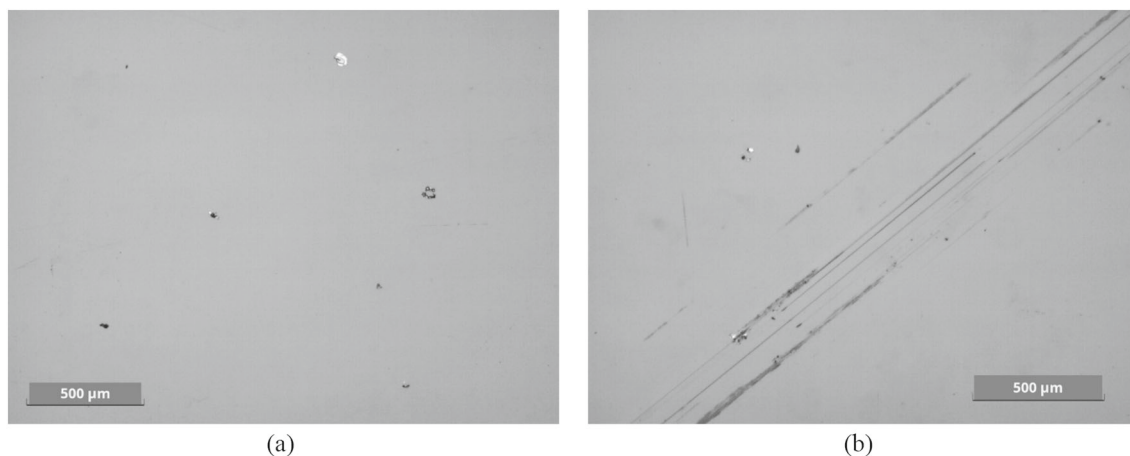
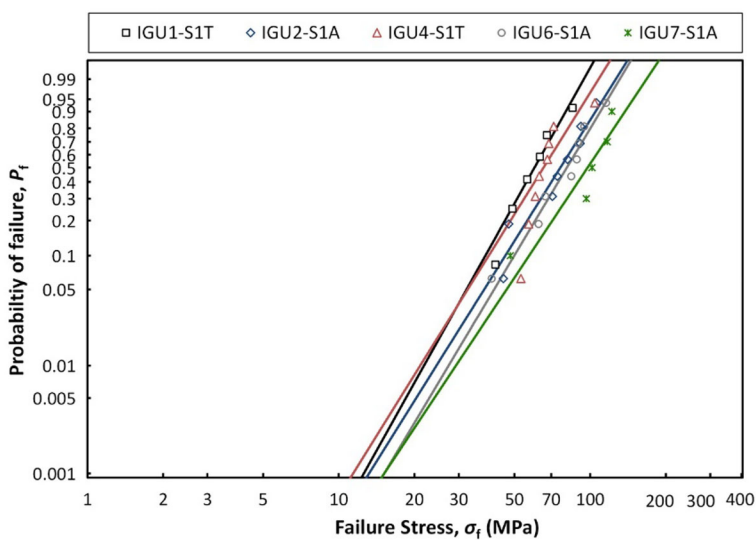


Fig. 7 Micrographs of externally facing glass surface (S1); **a** predominant pitting damage; **b** pits and scratches

Table 3 Weibull statistics and fracture strength for externally facing glass (surface S1)

Series	Goodness of fit, p_{AD} (%)	Weibull parameters		Coeff. of variation (%)	60s equivalent fracture strength			
		Shape factor β	Scale factor θ (MPa)		min σ (MPa)	max σ (MPa)	$\sigma_{f,0.008}$ (MPa)	$\sigma_{f,0.5}$ (MPa)
IGU1-S1T	74.56	4.19	65.51	26.91	41.96	85.02	20.70	60.02
IGU2-S1A	63.51	3.73	83.93	29.86	45.13	105.81	23.05	76.09
IGU4-S1T	2.23	3.75	71.87	29.72	53.00	104.32	19.87	65.18
IGU6-S1A	67.07	3.91	88.65	28.63	40.53	115.58	25.82	80.72
IGU7-S1A	27.69	3.51	108.36	31.54	48.10	121.96	27.44	97.63

Fig. 8 Cumulative distribution functions for externally facing glazing (surface S1)



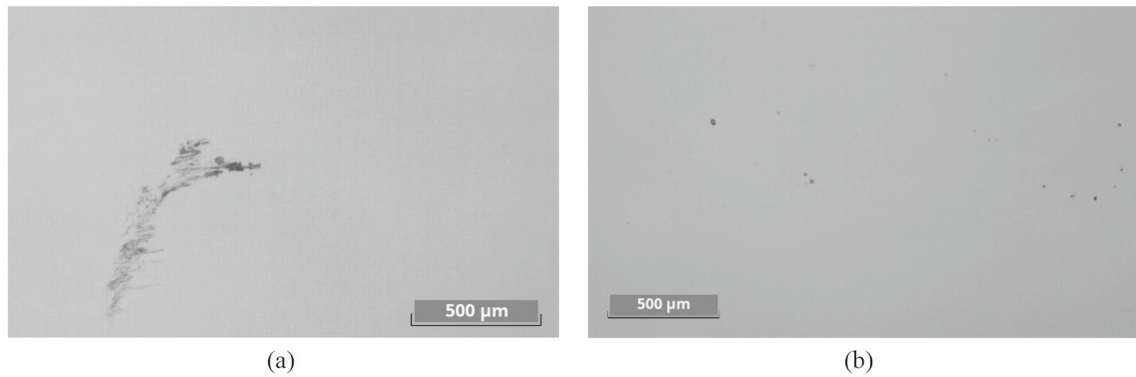


Fig. 9 Micrographs of cavity facing glass surface, with rare damage found on: **a** surface S2; **b** surface S3

Table 4 Weibull statistics and fracture strength for cavity facing glass for surfaces: (a) S2 and (b) S3

Series	Goodness of fit, p_{AD} (%)	Weibull parameters		Coeff. of variation (%)	60s equivalent fracture strength			
		Shape factor β	Scale factor θ (MPa)		$\min\sigma$ (MPa)	$\max\sigma$ (MPa)	$\sigma_{f,0.008}$ (MPa)	$\sigma_{f,0.5}$ (MPa)
(a)								
IGU3-S2A	59.58	6.82	135.83	17.22	108.11	157.65	66.92	128.72
IGU5-S2T	51.75	3.25	129.97	33.78	80.39	172.71	29.52	116.12
(b)								
IGU1-S3T	67.54	7.38	88.66	15.99	56.82	101.57	46.12	84.37
IGU4-S3A	83.10	2.13	137.30	49.40	44.55	206.07	14.25	115.59

accompanied by a wide range of fracture strength data of $45 \leq \sigma_f \leq 206$ MPa and $80 \leq \sigma_f \leq 173$ MPa, respectively. These shape factors were even smaller compared to those reported for externally facing glazing in Sect. 3.1. The cavity facing surfaces remained protected within the IGUs against flaw inducing mechanisms during transportation, installation and their service life. Consequently, uniformity in fracture strength data was instead expected. As mentioned, flaws introduced during assembly and/or disassembly of the IGUs could be potentially the underlying reason behind this discrepancy. Additionally, in the case of series IGU5-S2T, this could be also linked with flaws induced due to contact with the tin bath during the float process. Further future post fracture microscopy is essential for characterizing critical flaws in these series to fully understand the reasons behind this deviation.

Overall, the strength of glass at low probabilities of failure ($P_f = 0.008$) varied between $30 \leq \sigma_{f,0.008} \leq 67$ MPa for S2 and $14 \leq \sigma_{f,0.008} \leq 46$ MPa for S3 (Fig. 10). The upper limit of these series matches

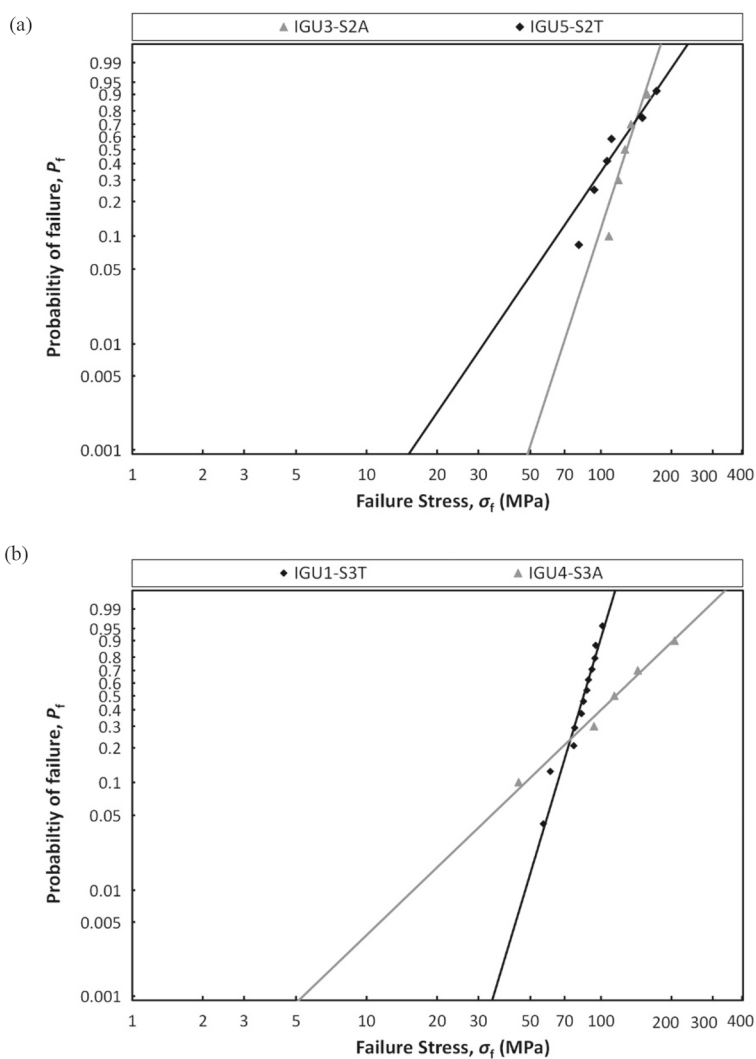
the bending strengths of glass reported in Datsiou and Overend (2017b) and Overend and Louter (2015), however, the lower end indicates that more severe damage was evident in the glass specimens of this study. Meanwhile, the mean fracture strength ranged between $116 \leq \sigma_{f,0.5} \leq 129$ MPa for S2 and $84 \leq \sigma_{f,0.5} \leq 116$ MPa for S3.

3.3 Internally facing glass surface

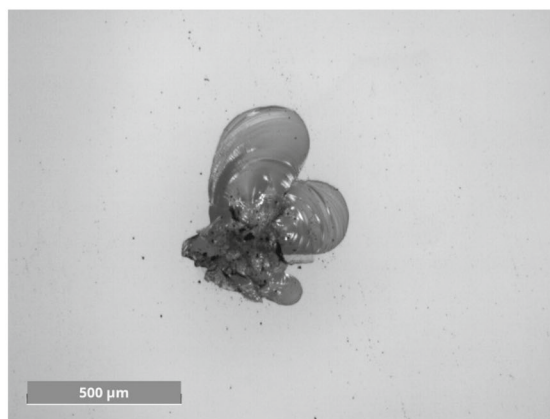
On the internally facing glass surface (S4 in Fig. 2), significant damage was observed, predominantly scratches (Fig. 11a), likely caused by cleaning, and some severe local pits (Fig. 11b), which might have been caused by an impact with a hard object during installation, use or dismantling and disassembly.

Five series of test data were analysed for internally facing glass surfaces derived from five distinct IGUs (Table 1). Fracture data were obtained from the tin side

Fig. 10 Cumulative distribution functions for cavity facing glass surfaces: **a** S2 and **b** S3



(a)



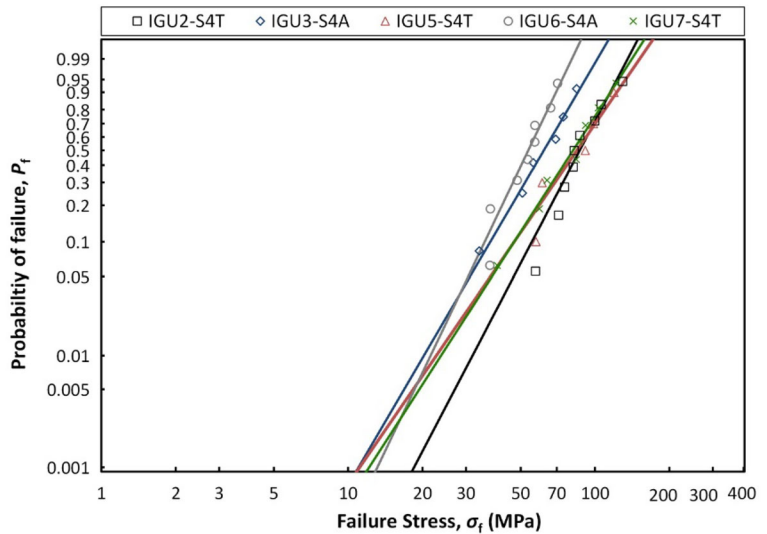
(b)

Fig. 11 Micrographs of the internally facing glass surface S4: **a** scratches and **b** pits

Table 5 Weibull statistics analysis and fracture strength for internally facing glass surface S4

Series	Goodness of fit, P_{AD} (%)	Weibull parameters		Coeff. of variation (%)	60s equivalent fracture strength			
		Shape factor β	Scale factor θ (MPa)		min σ (MPa)	max σ (MPa)	$\sigma_{f,0.008}$ (MPa)	$\sigma_{f,0.5}$ (MPa)
IGU2-S4T	53.71	4.23	94.53	26.65	57.44	129.43	30.25	86.69
IGU3-S4A	82.97	3.78	68.32	29.49	34.02	84.32	19.10	62.02
IGU5-S4T	59.42	3.23	94.58	34.02	57.73	119.42	21.23	84.43
IGU6-S4A	67.90	4.65	58.03	24.48	37.53	70.58	20.56	53.63
IGU7-S4T	82.19	3.44	90.58	32.13	40.17	121.98	22.29	81.43

Fig. 12 Cumulative distribution functions for internally facing glass surface S4



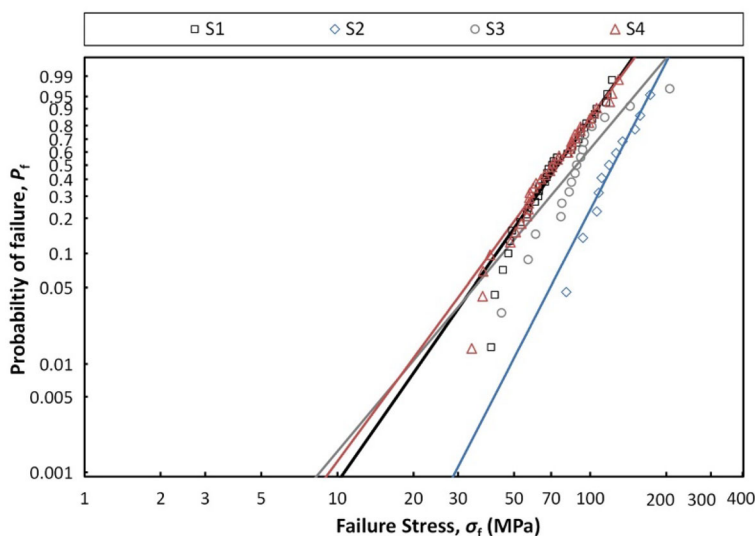
of glass for series IGU2-S4T, IGU5-S4T and IGU7-S4T while series IGU3-S4A and IGU6-S4A featured data from the air side of glass. All series were successfully fitted to a two parameter Weibull distribution, meeting the selected goodness of fit criteria (Table 5).

It was found that the shape factor, β , of the Weibull distribution was low and ranged for all series between $3.2 \leq \beta \leq 4.7$. This range was in close agreement with the one reported for the externally facing glazing, indicating that large variability in data was also apparent in this case. Although internally facing glazing was protected from outdoor elements during its service life, such as wind-borne projectiles, it was nonetheless subjected to ageing mechanisms stemming from normal indoor use and cleaning. These processes could have resulted in the induction of flaws that were randomly dispersed on the glazing surface.

CDFs for series IGU5-S4T and IGU7-S4T featuring tin side data, were almost identical (Fig. 12). However, the CDF for IGU2-S4T intersected the other two at approximately $P_f = 0.55$ and diverged considerably at low probabilities of failure. A fairly good agreement was found for the air series IGU3-S4A and IGU6-S4A although some discrepancy was observed at high probabilities of failure. It is worth noting that all series, irrespective of the side of glass used for acquiring the data, met at low probabilities of failure except for IGU2-S4T. Overall, the strength of glass varied between $19.1 \leq \sigma_{f,0.008} \leq 30.3$ MPa at low probabilities of failure ($P_f = 0.008$) with a coefficient of variation of 19.3% while the mean fracture strength ranged between $53.6 \leq \sigma_{f,0.5} \leq 86.7$ MPa with a coefficient of variation of 20.2%.

Table 6 Weibull statistics analysis and fracture strength for externally facing glazing (S1), cavity facing glazing (S2 and S3) and internally facing glazing (S4)

Series	Goodness of fit, p_{AD} (%)	Weibull parameters		Coeff. of variation (%)	60s equivalent fracture strength			
		Shape factor β	Scale factor θ (MPa)		min σ (MPa)	max σ (MPa)	$\sigma_{f,0.008}$ (MPa)	$\sigma_{f,0.5}$ (MPa)
S1	44.49	3.36	83.14	32.81	40.53	121.96	19.80	74.60
S2	73.31	4.55	133.58	24.96	80.39	172.71	46.26	123.24
S3	0.83	2.80	100.65	38.67	44.55	206.07	17.97	88.30
S4	59.50	3.18	81.79	34.52	34.02	129.43	17.92	72.88

Fig. 13 Cumulative distribution functions for externally facing glazing (S1), cavity facing glazing (S2 and S3) and internally facing glazing (S4)

3.4 Overall comparison

Fracture strength data for each of the four investigated surfaces, namely, externally facing glazing (S1), cavity facing glazing (S2 and S3) and internally facing glazing (S4) were grouped for all tested IGUs and were subsequently statistically analysed to allow direct comparison across different surfaces. Acceptable goodness of fit was noted for series S1, S2 and S4 (Table 6). S3 failed to conform to the selected goodness of fit criteria, although a visual inspection suggests a better fit to a bi-modal Weibull distribution (Fig. 13). Consequently, series S3 is excluded from further discussion in this section.

Interestingly, very close agreement was found for CDFs of series S1 and S4 (Fig. 13) indicating that the externally and internally facing surfaces experienced

similar levels of ageing during their service life. However, further post fracture microscopy is required to determine and compare the type and morphology of critical flaws found on both surfaces. As anticipated, the CDF of the protected, cavity facing surface, S2, was shifted along the horizontal axis towards higher strength values compared to surfaces S1 and S4. The coefficient of variation for surfaces S1 and S4 was very similar (32.8% and 34.5% respectively) whilst a lower coefficient of variation of 25% was found for S2.

Strengths at low probabilities of failure ($P_f = 0.008$) were found to be 19.8 MPa and 17.9 MPa for externally and internally exposed surfaces S1 and S4 respectively, indicating a 11% higher strength for externally facing glazing. In turn, the cavity facing surface exhibited a strength of 46.3 MPa at $P_f = 0.008$, denoting a 234% and 259% increase compared to exposed surfaces S1

and S4 respectively. This increase is attributed to the fact that surface S2 remained shielded from ageing within the IGU during its service life.

Observed strengths at low probabilities of failure, which correspond to design strength used in engineering applications, present a considerable potential for reuse. Design strength of new annealed glass under a 60s-load, calculated according to EN 16612:2019 (CEN 2019) for infill panels (consequence class CC0), equals 21.4 MPa. In comparison, surfaces S1 and S4 reach 93% and 84% of the design strength of new glass, respectively, while the surface S2 even exceeds it by a factor of 2. However, it should be noted that the tested surface was relatively small, potentially resulting in higher strengths due to the size effect. While the strength of the externally facing surface may not exhibit significant size dependence due to its highly dense and uniformly distributed damage, the specimen size might be a relevant factor for determination of the design strength of the cavity facing and internally facing surfaces, where a presence of more singular defects was observed (Veer et al. 2023).

With a possibility of non-destructive pre-detection of critical flaws and exclusion of potential outliers, the strength achievable with reused glass might be greater. The surface microscopy applied in this study proved to be limited in this respect. However, a number of tools and methodologies for glass surface quality assessment are currently in development, which can further facilitate the reuse of glass, such as optical scanner (Rota et al. 2023), optical profilometer (Veer et al. 2023) and non-linear acoustic method (Karlsson et al. 2023).

The applied test method with particularly small test surface area ($D_L/D_S = 18\text{ mm}/90\text{ mm}$), although yielding a higher number of specimens per glass pane/test series, resulted in a high number of invalid tests, i.e. specimens which failed outside the loading ring (Table 2). Percentage of valid tests ranged from 36% (IGU3-S2A) to 86% (IGU1-S3T), with an average of 52%, significantly reducing the data sets for statistical analysis. This puts in question the feasibility of the EN 1288-5 test method for the (comparative) analysis of the bending strength of aged glass. As observed by Rota et al. (2023), a larger test surface area (e.g. $D_L/D_S = 80\text{ mm}/150\text{ mm}$) increases the probability of detecting a critical defect, resulting in a higher percentage of valid tests with a fracture origin within or directly under the loading ring, which can also have an influence on the dispersion of the strength data.

4 Conclusions

The present study examined the surface quality of seven IGUs retrieved from a refurbishment project after 30 years of service life, focusing on the comparison of the four IGU glass surfaces. Qualitative assessment through microscopy revealed that glass quality was best preserved on the cavity-facing surface, which consequently exhibited the highest bending strength. The internally and externally facing surfaces, with visibly more extensive damage, exhibited similarly lower strengths at low probabilities of failure. When compared to the design strength of new annealed glass acc. to EN 16612, all the surfaces showed a reuse potential, with considerable bending strength.

Strengths at low probabilities of failure, which correspond to design strengths used in engineering applications, were found to be 19.8 MPa and 17.9 MPa for externally and internally exposed surfaces S1 and S4 respectively. This indicates a 10% higher strength for externally facing glazing, contrary to the expectation that externally facing glazing suffers the highest level of weathering. Further post fracture microscopy is required to determine and compare the type and morphology of critical flaws found on both surfaces. As anticipated, the cavity facing surface exhibited a 234% and 259% increase in strength at low probabilities of failure compared to exposed surfaces S1 and S2, respectively, reaching a strength of 46.3 MPa. This increase is attributed to the fact that surface S2 remained shielded from ageing within the IGU during its service life.

Acknowledgements Civil engineering students Abdullah Emin Buyrukoglu, Shalva Esakia, Leander Somann, and Jovanka Kuzmanovska from the Faculty of Civil Engineering — TU Dresden, are gratefully acknowledged for assisting the experimental work in this study. The authors would also like to thank Buijs Glas and Hemubo BV for the assistance in sourcing the used window glazing, and AGC Glass Europe for their support in determining the age of the IGUs based on the spacer code.

Funding Open Access funding enabled and organized by Projekt DEAL.

Data availability The fracture strength data sets generated during the current study are available from the corresponding author on reasonable request.

Declarations

Conflict of interest On behalf of all authors, the corresponding author states that there is no conflict of interest.

Open Access This article is licensed under a Creative Commons Attribution 4.0 International License, which permits use, sharing, adaptation, distribution and reproduction in any medium or format, as long as you give appropriate credit to the original author(s) and the source, provide a link to the Creative Commons licence, and indicate if changes were made. The images or other third party material in this article are included in the article's Creative Commons licence, unless indicated otherwise in a credit line to the material. If material is not included in the article's Creative Commons licence and your intended use is not permitted by statutory regulation or exceeds the permitted use, you will need to obtain permission directly from the copyright holder. To view a copy of this licence, visit <http://creativecommons.org/licenses/by/4.0/>.

References

- ASTM Standard C1499-09: Standard test method for monotonic equibiaxial flexural strength of advanced ceramics at ambient temperature. American Society for Testing and Materials, West Conshohocken, PA (2013). <https://doi.org/10.1520/C1499-09R13>
- ASTM Standard E1300-16: Standard practice for determining load resistance of glass in buildings. American Society for Testing and Materials, West Conshohocken, PA (2016). <https://doi.org/10.1520/E1300-16>
- Bristogianni, T., Oikonomopoulou, F.: Glass up-casting: a review on the current challenges in glass recycling and a novel approach for recycling “as-is” glass waste into volumetric glass components. *Glass Struct. Eng.* **8**, 255–302 (2023). <https://doi.org/10.1007/s40940-022-00206-9>
- Brown, W. G.: A load duration theory for glass design. In: Annual Meeting of the International Commission on Glass, pp. 75–78 (1969)
- CEN (European Committee for Standardisation): EN 1288-5: 2000 Glass in building - Determination of the bending strength of glass—part 5: coaxial double ring test on flat specimens with small test surface areas (2000)
- CEN (European Committee for Standardisation): EN 16612:2019 glass in building. Determination of the lateral load resistance of glass panes by calculation (2019)
- CWCT (Centre for Window and Cladding Technology): Sustainability Guide 01: an introduction to sustainability in Façades. CWCT (2021)
- Datsiou, K.C., Overend, M.: Artificial ageing of glass with sand abrasion. *Constr. Build. Mater.* **142**, 536–551 (2017a). <https://doi.org/10.1016/j.conbuildmat.2017.03.094>
- Datsiou, K.C., Overend, M.: The strength of aged glass. *Glass Struct. Eng.* **2**(2), 105–120 (2017b). <https://doi.org/10.1007/s40940-017-0045-6>
- Datsiou, K.C., Overend, M.: Weibull parameter estimation and goodness-of-fit for glass strength data. *Struct. Saf.* **73**, 29–41 (2018). <https://doi.org/10.1016/j.strusafe.2018.02.002>
- DP6 architectuurstudio: The Natural Pavilion, Floriade Expo 2022. <https://www.dp6.nl/en/projecten/the-natural-pavilion-floriade-2022> (2024). Accessed 14 March 2024
- European Commission: A Clean Planet for all—A European strategic long-term vision for a prosperous, modern, competitive and climate neutral economy, COM/2018/773 final. <https://eur-lex.europa.eu/legal-content/EN/TXT/?uri=CELEX%3A52018DC0773> (2018). Accessed 8 March 2024
- European Commission: A Renovation Wave for Europe—greening our buildings, creating jobs, improving lives, COM/2020/662 final. <https://eur-lex.europa.eu/legal-content/EN/TXT/?uri=CELEX%3A52020DC0662> (2020). Accessed 8 March 2024
- Forslund, H., Björklund, M.: Toward circular supply chains for flat glass: challenges of transforming to more energy-efficient solutions. *Energies* **15**(19), 7282 (2022). <https://doi.org/10.3390/en15197282>
- Geboes, E., Galle, W., De Temmerman, N.: Make or break the loop: a cross-practitioners review of glass circularity. *Glass Struct. Eng.* **8**, 193–210 (2023). <https://doi.org/10.1007/s40940-022-00211-y>
- GSF Glasgroep: Range of circular glazing—isoMAX circular glazing. <https://isomax.nl/en/assortiment/> (2024). Accessed 14 March 2024
- Haldimann, M.: Fracture strength of structural glass elements - analytical and numerical modelling , testing and design. PhD Thesis, École Polytechnique Fédérale de Lausanne (EPFL) (2006). <https://doi.org/10.5075/epfl-thesis-3671>
- Hartwell, R., Coult, G., Overend, M.: Mapping the flat glass value-chain: a material flow analysis and energy balance of UK production. *Glass Struct. Eng.* **8**, 167–192 (2023). <https://doi.org/10.1007/s40940-022-00195-9>
- Karlsson, S., Kozłowski, M., Grund, L., Andersson, S.A.K., Haller, K.C.E., Persson, K.: Non-destructive strength testing of microindented float glass by a nonlinear acoustic method. *Constr. Build. Mater.* **391**, 131748 (2023). <https://doi.org/10.1016/j.conbuildmat.2023.131748>
- Overend, M., Louter, C.: The effectiveness of resin-based repairs on the inert strength recovery of glass. *Constr. Build. Mater.* **85**, 165–174 (2015). <https://doi.org/10.1016/j.conbuildmat.2015.03.072>
- Rose, A., Sack, N., Nothacker, K., Gassman, A.: Recycling of flat glass in the building industry - Analysis of the current situation and derivation of recommendations for action. ift Rosenheim. https://www.irbnet.de/daten/kbf/kbf_e_F_3202.pdf (2019). Accessed 8 March 2024
- Rota, A., Zaccaria, M., Fiorito, F.: Towards a quality protocol for enabling the reuse of post-consumer flat glass. *Glass Struct. Eng.* **8**, 235–254 (2023). <https://doi.org/10.1007/s40940-023-00233-0>
- Stuurstraat, N.: Strength of naturally aged glass units determined by experimental testing: Glass Reuse. Master thesis, TU Delft. <http://resolver.tudelft.nl/uuid:1f5681dc-785e-4f1f-b047-499c83ddc46d> (2023). Accessed 8 March 2024
- van Nieuwenhuijzen, E.J., Tetteroo, J.I.A., van de Vliet, M., Melet, E.: In situ detection of product age and argon concentration as measure of the re-use potential of insulating glass

units in buildings. *Glass Struct. Eng.* **8**, 211–233 (2023). <https://doi.org/10.1007/s40940-023-00225-0>

Veer, F., Overend, M., Sofokleous, I., Noteboom, C.: A Novel method for the non-destructive assessment of strength degradation and re-use potential of weathered float glass from facades: a proof of concept study. *Int. J. Struct. Glass Adv.* **7**(1), 1–15 (2023). <https://doi.org/10.3844/sgamrsp.2023.1.15>

Publisher's Note Springer Nature remains neutral with regard to jurisdictional claims in published maps and institutional affiliations.